Journal of Materials Chemistry

Dynamic Article Links

Cite this: J. Mater. Chem., 2012, 22, 13159

www.rsc.org/materials

PAPER

ZnO@silica core–shell nanoparticles with remarkable luminescence and stability in cell imaging†

Hua-Juan Zhang,[a] Huan-Ming Xiong,*[b] Qing-Guang Ren,*[a] Yong-Yao Xia[b] and Ji-Lie Kong[c]

Received 12th February 2012, Accepted 8th May 2012
DOI: 10.1039/c2jm30855j

Monodispersed silica-coated ZnO nanoparticles were successfully synthesized and modified with hydrophilic amino groups on the surfaces. The emission colour of the as-prepared ZnO nanoparticles could be tuned by adjusting the reactant ratio and the reaction time. The resulting particles were stable in water, phosphate buffer saline and cell culture medium. Their aqueous solutions had high quantum yields of 53.8%, 48.7% and 33.5%, corresponding to blue, green and yellow emitting ZnO@silica nanoparticles respectively. And the cytotoxicity (24 hours LC50 for Hela cells) of these three samples was 315, 374 and 241 μg mL^{-1} respectively. The cytotoxicity data and the cellular uptake kinetics experiments confirmed the safety of all these ZnO@silica nanoparticles under visible light, while under UV light of 365 nm the yellow emitting ZnO@silica was fatal to Hela cells because it released plenty of reactive oxygen species.

1. Introduction

In the past decade, quantum dots have received great attention as biological labelling agents due to their distinguished luminescent properties such as high quantum yield, narrow and symmetric emission spectra, especially their size-dependent emission.[1–3] Since the classical CdSe and CdTe quantum dots may cause serious harm to animals, human beings and the environment by releasing toxic Cd^{2+} ions and reactive oxygen species (ROS),[3–8] scientists are testing other low toxicity nanoparticles as candidates. ZnO is a kind of cheap, environmentally friendly and biocompatible material and listed as safe matter by the US Food and Drug Administration (21CFR182.8991). Hence, photoluminescent ZnO nanoparticles (NPs) are promising alternative materials for biomedical application.

ZnO NPs with visible emission can be produced simply by sol–gel methods.[9,10] But without surface modification, they are not stable in water because their luminescent centers on the surface can be destroyed rapidly by water.[4,11] In order to prevent ZnO NPs from fluorescence quenching and Zn^{2+} ions leaching, various surface coating have been reported. It has been found that the decomposed ZnO NPs are toxic mildly to organisms,[12–16] and the Zn^{2+} concentration has significant correlations with the cell viability and the lactate dehydrogenase (LDH) level.[17] Recent studies pointed out that not only Zn^{2+} ions but also surface chemistry, especially ROS generation from ZnO NPs, plays a crucial role in ZnO toxicity.[17–20] By far, it is still a great challenge to develop convenient methods of synthesizing ZnO NPs that are surface functionalized, stable in biological mediums, low in toxicity and highly luminescent.

Recently, some researchers synthesized water-stable ZnO NPs *via* one-pot polyol hydrolysis route, using triethylene glycol as reaction agent.[21,22] However, these ZnO NPs had only blue emission that is less favourable for biomedical imaging because many cells also emit blue light upon UV irradiation. Fu and co-workers prepared water-stable ZnO NPs with very high quantum yield, but the products exhibited only blue emission and this emission was not from ZnO NPs themselves.[23] Our research group has successfully prepared stable aqueous ZnO NPs with green and yellow emission through co-polymerization on ZnO surface. Such ZnO NPs had the internal hydrophobic polyester shells and the outside hydrophilic polyether groups, and they showed low toxicity to cancer cells.[24] But they had no functional groups to be conjugated with bioactive molecules, and they were not very stable in phosphate buffer saline (PBS) and culture medium. Lately, Saliba and co-workers modified ZnO NPs using hyperbranched polymers which had amino groups. The products were stable in several solvents, but not tested in buffer solution and culture medium. Moreover, the quantum yield of the ZnO NPs was only about 5%, indicating that these ZnO materials were not fit for bioimaging.[25]

[a]*Center of Analysis and Measurement, Fudan University, 220 Hand Road, Shanghai 200433, P. R. China. E-mail: qgren@fudan.edu.cn*
[b]*Department of Chemistry and Shanghai Key Laboratory of Molecular Catalysis and Innovative Materials, Fudan University, 220 Hand Road, Shanghai 200433, P. R. China. E-mail: hmxiong@fudan.edu.cn*
[c]*Department of Chemistry and Institutes of Biomedical Sciences, Fudan University, 220 Hand Road, Shanghai 200433, P. R. China*

† Electronic supplementary information (ESI) available: Quantum yield evaluation of ZnO@silica samples, photoluminescent spectra of ZnO@silica in different media, the cellular uptake kinetics experiments observed by a laser scanning confocal microscope and the amplified HRTEM images of the ZnO@silica samples. See DOI: 10.1039/c2jm30855j

Silica is often selected as the shell material for NPs because of its biocompatibility and protection effects.[26–29] On one hand, silica shells impede diffusion of chemicals between the inside and outside of NPs, and thus lower the toxic effect of the NPs toward cells and in the meantime, improve chemical and photochemical stabilities of the quantum dots.[30] On the other, silica shells provide rich surface chemistry in bioconjugation that is important for biomedical application. Although numerous methods have been reported for coating silica onto NPs,[30–45] only a few articles have discussed silica-coated ZnO NPs.[11,41–45]

Jana and co-workers reported the preparation of stable ZnO colloidal solutions through a two-step surface silanization, using trialkoxysilanes or trihydroxysilanes as silanization agent. Their ZnO NPs had diameters of about 5 nm and quantum yields of 16–20%. But the luminescence intensity of the products was significantly reduced under the continuous UV excitation.[11] Wang *et al.* prepared monodispersed silica coated ZnO NPs in microemulsion system, using PVP as the capping agent. The products were 24–50 nm multicore particles without any luminescence data.[41] None of the above reports provided cytotoxicity data. Moussodia and co-workers modified ZnO NPs by using poly(ethylene glycol)-siloxane covalently linked to the ZnO surface to make these nanoparticles water dispersible, but the product quantum yield showed a significant decrease after surface ligand exchange, from 18% to 8% after silanization.[42] Later, they coated ZnO NPs by poly(amidoamine) (PAMAM) dendrons with a siloxane group. The quantum yield of the final products in water was improved to about 18%. The cytotoxicity test on *Escherichia coli* verified the biocompatibility of such ZnO–PAMAM, but the stability of the products in PBS and culture mediums was not mentioned.[43] Tang *et al.* prepared multicore ZnO@silica NPs with the average size of 50 nm. The products were stable in water and PBS, but the stability data in culture mediums were not reported. Such ZnO@silica NPs had mild cytotoxicity and could be successfully attached to the cell surface, although the quantum yield decreased after silica modification.[44] The latest work by Shi *et al.*[45] reported ZnO NPs modified with (3-(2,3-epoxy-propoxy)propyl)trimethoxysilane (KH560). The quantum yields of the products were higher than 30%, and such KH560 modified ZnO NPs are ultrastable in ethanol. However, this report has neither stability data in water, nor biological experiments.

According to the above review of literature, it is really difficult to obtain highly luminescent ZnO@silica NPs with good stability in water, buffer solution and cell culture medium. Moreover, there was no report concerning the cellular uptake processes and luminescence stability of ZnO NPs with cells in culture medium. Our present work will focus on these aspects so as to pave a way for ZnO NPs in biological applications. Here, we show a kind of monodispersed ZnO@silica core–shell NPs with remarkable quantum yield and excellent stability in water, PBS and Roswell Park Memorial Institute (RPMI) Medium 1640. Amino groups were modified on the surface of the ZnO@silica for further bioconjugation. Cytotoxicity tests showed the products had mild toxicity to Hela cells. After cellular uptaking, the ZnO@silica nanoparticles showed excellent luminescence stability in RPMI Medium 1640 under continuous UV irradiation.

2. Experimental section

Preparation of ZnO NPs

ZnO NPs were prepared on the basis of our previous method[46] with slight modifications. The ZnO powder and methacrylic acid (MAA) were used as received from Sinopharm Chemical Reagent Co., Ltd. Methacrylic acid (MAA) was mixed with deionized water by a volume ratio of $MAA : H_2O = 1 : 4$, heated to 60 °C and then reacted with appropriate amount of ZnO powder under stirring for about 1 hour to get zinc methacrylate ($Zn(MAA)_2$). The unreacted ZnO powder was removed by filtration. Such zinc methacrylate aqueous solution was concentrated and dried by rotary evaporation at 70 °C and then dehydrated in a vacuum oven at 80 °C for 24 hours. 2.35 g of anhydrous $Zn(MAA)_2$ was dissolved in 100 mL of absolute ethanol and the solution was refluxed for about 1 hour at 80 °C. 1.26 g or 0.63 g of $LiOH \cdot H_2O$ was dissolved in 100 mL of absolute ethanol by sonication and then mixed with $Zn(MAA)_2$ ethanol solution respectively. After 24 hours at room temperature, the solution was concentrated by a rotation evaporator at 40 °C and then ZnO NPs were precipitated by adding excess ethyl acetate. Afterwards, ZnO NPs separated by centrifugation was dissolved in 200 mL of absolute ethanol. The blue-emitting ZnO NPs (designated as ZnO-A) and green-emitting ZnO NPs (designated as ZnO-B) were derived from 1.26 g and 0.63 g of $LiOH \cdot H_2O$ respectively. To obtain yellow-emitting ZnO NPs (designated as ZnO-C), ZnO-B was synthesized first and then stored at room temperature for 20 days.

Preparation of ZnO@silica

50 mL of ZnO ethanol colloid was diluted with another 50 mL of ethanol, stirred and heated at 70 °C for 10 min. And then 0.2 mL of vinyltriethoxysilane (VTES) and 0.032 g of 2,2′-azobisisobutyronitrile (AIBN) were added into the above solution and refluxed for 30 min. Subsequently, the mixture was concentrated by rotary evaporation at 40 °C and precipitated by ethyl acetate. The supernatant was discarded and the precipitate was dissolved in 100 mL of ethanol. 20 mL of the as-prepared ZnO–VTES NPs colloid was diluted by 20 mL of ethanol and then mixed with a solution containing 0.1 mL of TEOS and 20 mL of ethanol. Another solution composed of 0.05 mL of 25 wt% ammonia, 0.2 mL of H_2O and 20 mL of ethanol, was added slowly to the above solution with continuous stirring for 20 hours, followed by adding 0.05 mL of 3-aminopropylthiethoxysilane (APS). After stirring for another 10 hours, the solution was concentrated by rotary evaporation at 40 °C and precipitated with excess ethyl acetate again. The precipitate was separated by centrifugation and redispersed in 60 mL of ethanol. The solution was heated at 80 °C for 15 min and then placed at room temperature for 1 day. After another circle of concentration, precipitation and centrifugation procedure as described above, the final ZnO@silica products were dissolved in water, PBS or RPMI Medium 1640 respectively for further experiments. In the following part of this article, ZnO-A@silica stands for blue samples, ZnO-B@silica for green samples and ZnO-C@silica for yellow samples.

Cell viability measurement

Hela cells were cultured in RPMI Medium 1640 (Gibco BRL) supplemented with 10% fetal calf serum (FCS, Gibco BRL), penicillin 100 U mL^{-1}, streptomycin 100 μg mL^{-1} and 1% glutamine (Gibco BRL). An environment of humidified air containing 5% CO_2 was maintained at 37 °C. Cells were seeded in 96-well plates (Gibco BRL) at a density of 1×10^5 cells per mL for 1 day and then treated with different concentrations of ZnO@silica NPs (400, 200, 100, 50 and 25 μg mL^{-1} respectively) in RPMI Medium 1640 containing 10% FCS for 24 hours. After treatment, the medium was aspirated and 100 μL of fresh medium with 10% FCS was added to each well with a 3-(4,5-dimethylthiazol-2-yl)-2,5-diphenyl-2*h*-tetrazoliumbromide (MTT, Sigma) stock solution (10 μL, 5 mg mL^{-1}). Cells were cultured for 4 hours at 37 °C. Afterwards, the medium was removed, and the cells were lysed with dimethylsulfoxide (DMSO, 100 μL per well). The absorbance at 490 nm of each well was measured by a Molecular Devices SpectraMax M5 Microplate Reader. All experiments were done in quadruplicate and illustrated as average data with error bars. In each set of experiment, the data were expressed as relative survival rates as normalized to the untreated control. The untreated control was set as 100%.

ROS measurement

ROS was determined by ROS assay kit which contained 2′,7′-dichlorofluorescin diacetate (DCFH-DA). After entering the cell, DCFH-DA is hydrolyzed by the esterase to DCFH. And then nonfluorescent DCFH is oxidized to fluorescent compound dichlorofluorescein (DCF) by cellular oxidants. A DCFH-DA stock solution of 10 mM was diluted 1000-fold in the cell culture medium without serum to yield a 10 μM working solution. Hela cells were washed three times by cell culture medium without serum and then incubated with DCFH-DA working solution for 30 min in the dark environment (37 °C incubator). Afterwards, cells were washed three times by cell culture medium without serum to eliminate DCFH-DA that did not enter the cells. Then the cells were treated with 50 μg mL^{-1} ZnO@silica NPs, followed by exposure under 365 nm UV light or under visible light for 30, 60, 90, 120, 150 and 180 min. The fluorescence was determined by the Microplate Reader, using excitation wavelength at 488 nm and recording emission at 525 nm. All experiments were done in quadruplicate and the average data were illustrated with error bars.

Characterization

A JEM-2010 transmission electron microscope operating at 200 kV was employed to obtain High Resolution Transmission Electron Microscopy (HRTEM) images. The photoluminescence (PL) spectra and UV-Vis absorption data were recorded on a Varian Cary Eclipse fluorescence spectrophotometer and a Unico UV-2802 PC spectrometer respectively. Fourier transform infrared (FT-IR) spectra were recorded on Nicolet Nexus 470 FT-IR Spectrometer. Cellular fluorescent images and fluorescence intensity were recorded on a Leica TCS SP5 Laser Scanning Confocal Microscope. Hela cells were seeded in glass bottom cell culture dishes at a density of 1×10^5 cells per mL for 1 day and then mixed with ZnO@silica NPs and RPMI Medium 1640 without FCS, followed by exposure under the 365 nm UV light for 170 min at 37 °C. The control group without ZnO@-silica was treated under the same condition. The fluorescent images and the average fluorescence intensity of the cells were recorded at 10 minute intervals.

Statistical analysis

A statistical analysis of particle size distribution, quantum yield and ROS level was done by Origin 8.5. A statistical significant differences analysis of cytotoxicity data and ROS level was done by SPSS 16.0. One-way analysis of variance (ANOVA) was used to determine statistical significance between values. Statistical significance was accepted at $p < 0.05$. The cytotoxicity was presented as Lethal Concentration 50 (LC50) value on a compound basis, which were calculated by Microsoft Excel.

3. Results and discussion

Modification on ZnO surface was carried out through a three-step silanization as illustrated in Scheme 1. First, ZnO–MAA NPs prepared by hydrolyzing zinc methacrylate, which had MAA groups on their surfaces, could copolymerize with VTES in the presence of AIBN initiator and heating treatment. In this way, VTES was bound onto the ZnO surface to form a silica monolayer. Secondly, under NH_3/H_2O catalysis, the silica layer grew up by hydrolyzing TEOS. Finally, APS was used to graft amino groups onto the surface of the nanoparticles. After centrifugation and purification, the as-prepared ZnO@silica NPs could be redispersed in ethanol, water, PBS and cell culture respectively, forming clear colloids.

The HRTEM images in Fig. 1 and S5† showed that the ZnO@silica NPs were monodispersed with average diameters of 2.7, 3.8 and 4.4 nm for ZnO-A@silica, ZnO-B@silica and ZnO-C@silica respectively. Thus, the emission colours of our ZnO@silica NPs were typically size-dependent due to quantum size effect. The silica shells were not observed even under a higher resolution, suggesting that the surface silica layers were very thin and amorphous. In Fig. 2, the UV-Vis absorption spectra and photoluminescent (PL) spectra of three ZnO@silica colloids were compared. All of the ZnO NPs showed a broad absorption band with onset at 340–360 nm. According to Meulenkamp's experiential formula $1240/\lambda_{1/2} = a + b/D^2 - c/D$ (here, $\lambda_{1/2}$ represents the wavelength where the absorption is half of that at the absorption peak or shoulder; D represents the average size of ZnO nanoparticle; a, b and c are parameters when D is within the range 25–65 Å),[9,47] the particle size of three ZnO@silica samples was evaluated to be 2.5, 3.5 and 4.2 nm respectively. This result was in accordance with the observation by TEM. Previous investigations proved that oxygen vacancy is the dominant origin of ZnO visible emission,[4,48–50] and the polymer shell can impede chemicals diffusion to the surface of the inside nanoparticles. In general, a thin silica shell is not sufficient for protecting ZnO NPs because the silica shell usually has plenty of micropores. However in this work, after dispersion and storage in PBS and RPMI Medium 1640, the PL spectra of ZnO@silica NPs were similar with those in water (Fig. S2 and S3†). No precipitation was observed, indicating the good stability and solubility of

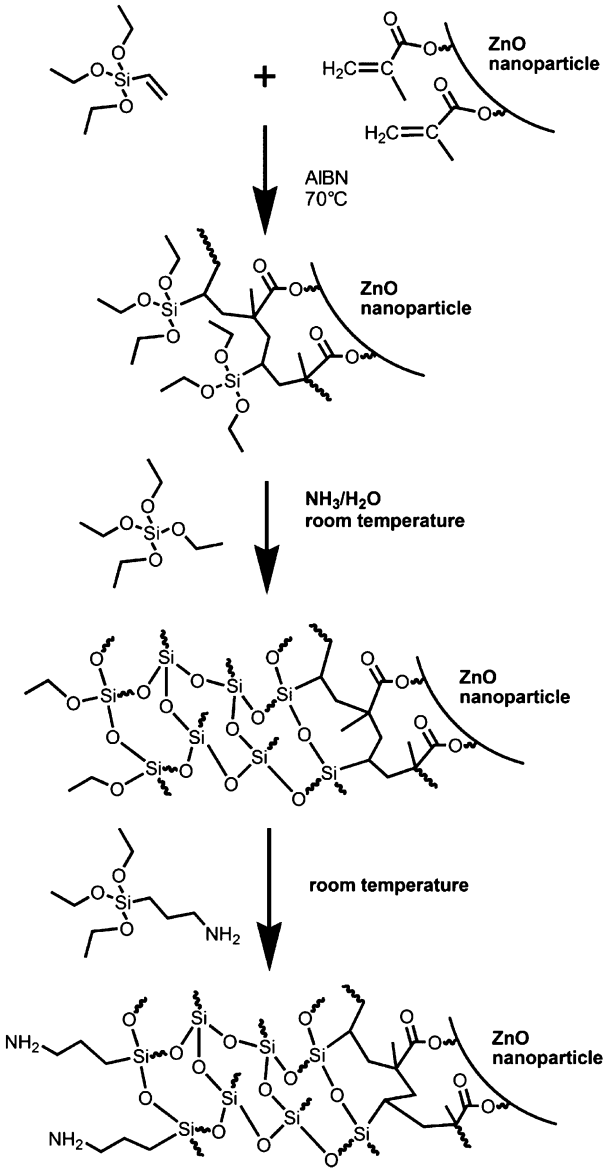

Scheme 1 Synthetic route for ZnO@silica NPs.

ZnO@silica NPs in both mediums. Such advantage can be ascribed to the three-step silanization which produces a tight and dense shell around ZnO NPs. The quantum yields of the blue, green and yellow emission were 53.8%, 48.7% and 33.5% respectively, as shown in Fig. S1†, which are significantly higher than those of other ZnO@silica nanoparticles in literature.[11,41–45] The fluorescence of three samples under UV light seemed very bright, ensuring their application as fluorescent probes.

The FT-IR spectra of the purified and dried ZnO@silica powder are shown in Fig. 3. The vibration bands observed at about 460 cm^{-1} in all spectra are attributed to the stretching mode of Zn–O bonds. The characteristic absorption of the Si–O–Si symmetrical stretching at about 1100 cm^{-1}, the Si–C bending at about 800 cm^{-1} and the Si–C stretching at about 1260 cm^{-1}, are proof of the silica shells, while N–H asymmetric stretching band at 3120–3600 cm^{-1} and N–H bending absorption band at about 1580 cm^{-1} prove the APS modification on ZnO surfaces.

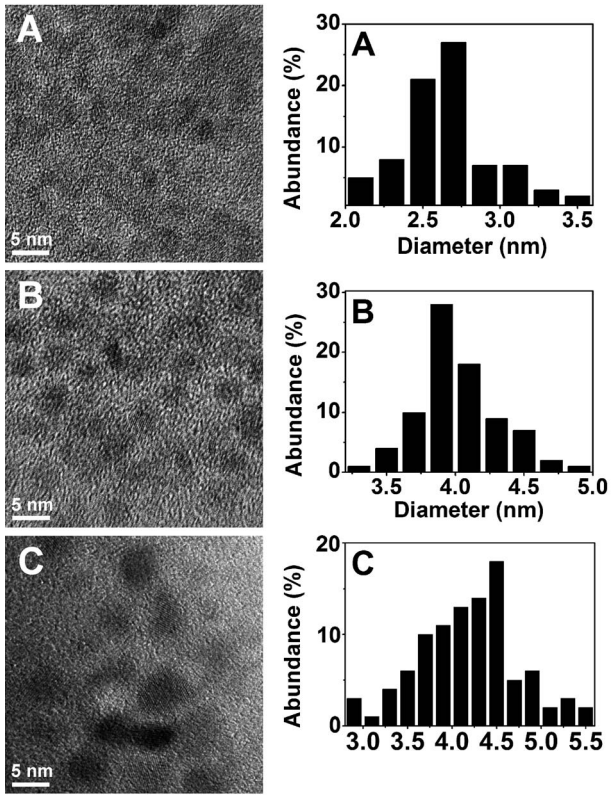

Fig. 1 HRTEM images (left) and size distribution graphs (right) of (A) ZnO-A@silica, (B) ZnO-B@silica and (C) ZnO-C@silica.

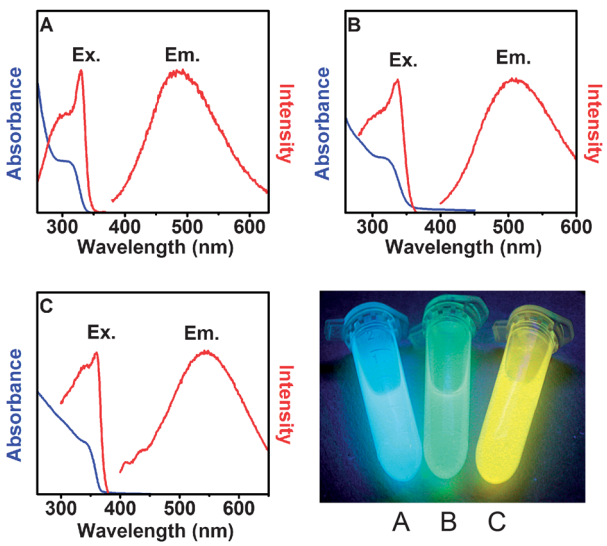

Fig. 2 Photoluminescent spectra (red) and absorption spectra (blue) of (A) ZnO-A@silica, (B) ZnO-B@silica and (C) ZnO-C@silica in water, with a photograph of these samples under a UV lamp. The PL emission spectra of sample A, B and C were recorded under 330, 340 and 360 nm excitation respectively, while their corresponding PL excitation spectra were obtained by 488, 513 and 550 nm detection.

After incubation with Hela cells for 24 hours, cytotoxicity results showed that the LC50 of ZnO-A@silica, ZnO-B@silica and ZnO-C@silica NPs were 315, 374 and 241 μg mL^{-1} respectively, suggesting that ZnO@silica NPs are quite safe to living

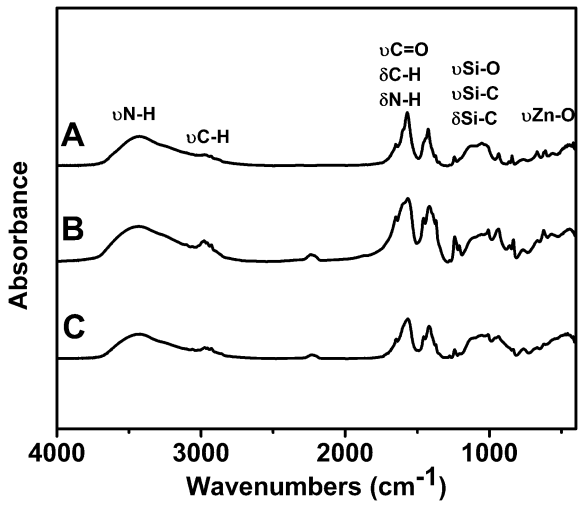

Fig. 3 FT-IR spectra of (A) ZnO-A@silica NPs, (B) ZnO-B@silica NPs and (C) ZnO-C@silica NPs.

cells *in vitro*. The cytotoxicity of ZnO-C@silica was significantly higher than those of ZnO-A@silica and ZnO-B@silica when the concentrations were above 50 μg mL^{-1}. But the cytotoxicity of ZnO-A@silica and ZnO-B@silica was similar with each other when the concentrations were below 400 μg mL^{-1} (Fig. 4). This result can be interpreted by the synthetic route. Before synthesizing ZnO-C@silica, ZnO-B NPs were stored for 20 days. During this period, ZnO NPs aggregated and grew larger, which might cause MAA ligand loss on ZnO surface and finally produced uncompleted shells. And thus, the ZnO core in sample C was apt to release more Zn^{2+} so as to show higher cytotoxicity than the other two samples.

In Fig. 5, these ZnO@silica NPs were tested as bio-imaging probe through Hela cellular uptake experiments. It is seen that

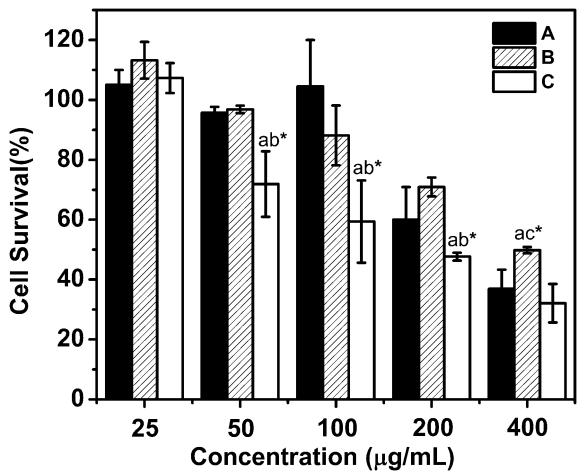

Fig. 4 Cytotoxicity toward Hela cells of (A) ZnO-A@silica NPs, (B) ZnO-B@silica NPs and (C) ZnO-C@silica NPs from a MTT assay. The significant difference was done by SPSS 16.0 and judged at $p < 0.05$. Significant difference is indicated by: ac* $p < 0.05$ *vs.* ZnO-A@silica NPs and ZnO-C@silica NPs treated cell groups; ab* $p < 0.05$ *vs.* ZnO-A@silica NPs and ZnO-B@silica NPs treated cell groups; a* $p < 0.05$ *vs.* ZnO-A@silica NPs treated cell groups.

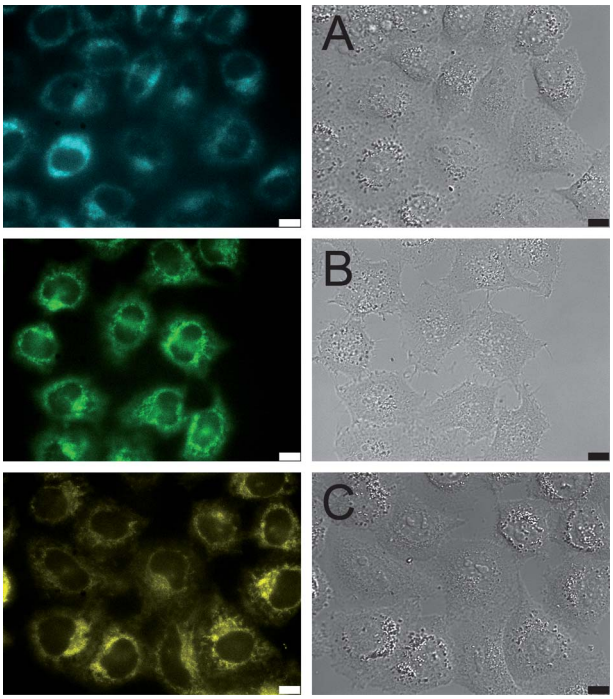

Fig. 5 Confocal luminescence images of Hela cells incubated with 50 μg mL^{-1} of (A) ZnO-A@silica NPs, (B) ZnO-B@silica NPs and (C) ZnO-C@silica NPs at 37 °C under UV light of 365 nm. The left pictures are fluorescent images of Hela cells while the right pictures are the corresponding DIC images. The bars in each picture represent 10 μm.

ZnO NPs mainly exist in the cytoplasm while the nucleus are not luminescent. Under the continuous UV irradiation, the fluorescence intensity of the Hela cells treated with ZnO@silica NPs gradually increased with time, suggesting gradual uptake of ZnO@silica NPs. But the fluorescence intensity didn't increase linearly with time (Fig. 6), which may result from electrodynamic interactions and steric interactions between ZnO@silica NPs and the cellular membrane surfaces, as well as the dissociation balance between nanoparticles and proteins. In the DIC pictures

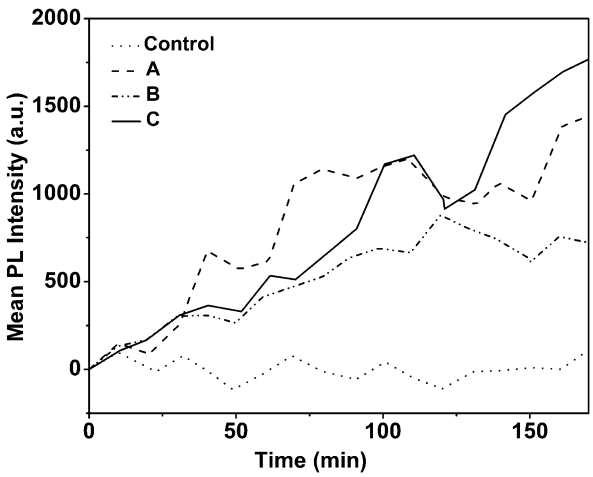

Fig. 6 Changes of fluorescence intensity of Hela cells treated with the control and (A) ZnO-A@silica NPs, (B) ZnO-B@silica NPs and (C) ZnO-C@silica NPs as a function of time.

(see Fig. S4†), some cells treated with ZnO-C@silica NPs formed blebs on the surface of cellular membrane after 100 min UV irradiation, but the cells treated with ZnO-A@silica NPs and ZnO-B@silica NPs showed no blebs within 170 min, as well as the control. These blebs can be ascribed to the ROS damage. Since the ZnO core in ZnO-C@silica NPs is more apt to release toxic Zn^{2+} which is associated with high levels of ROS production[17,51] and ZnO-C@silica NPs are easier to be excited by the 365 nm light than ZnO-A@silica and ZnO-B@silica, as the absorption data shown in Fig. 2, ZnO-C@silica NPs will produce much more ROS to destroy the cells.

In Fig. 6, the mean fluorescence intensities of the cells treated with different ZnO samples and the control are compared. The PL intensity of the sample A is higher than sample B and C within the initial 90 min, because ZnO-A@silica has the highest quantum yield and the smallest size. However, after 100 min continuous UV irradiation, the PL intensity of the sample C increased sharply, indicating plenty of ZnO-C@silica NPs have entered the cells. This phenomenon was accompanied by the emerging of membrane blebs as discussed above (see Fig. S4†), indicating that under continuous UV irradiation, the ROS produced by ZnO NPs damaged cellular membrane and induced rapid uptake of ZnO NPs, and thus, accelerated cell death.

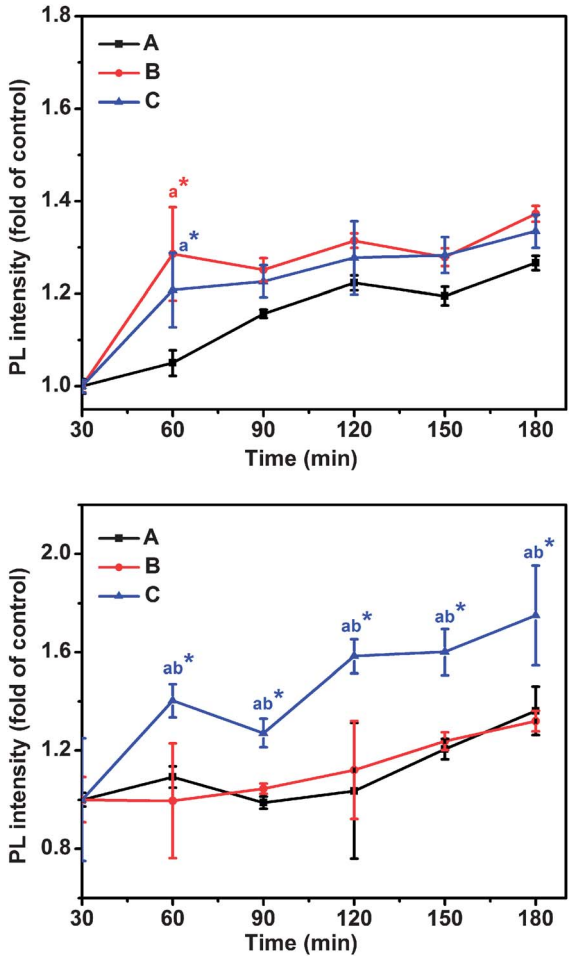

Fig. 7 ROS level of Hela cells induced by 50 μg mL^{-1} of (A) ZnO-A@silica, (B) ZnO-B@silica and (C) ZnO-C@silica treatment after exposure to visible light (upper) and UV light of 365 nm (below) for different time. ROS was detected by fluorescence measurement of DCF and the results are given in fold of the control groups. The significant difference was done by SPSS 16.0 and judged at $p < 0.05$. Significant differences are indicated by: ab* $p < 0.05$ *vs.* ZnO-A@silica NPs and ZnO-B@silica NPs treated cell groups; a* $p < 0.05$ *vs.* ZnO-A@silica NPs treated cell group.

Recently, Guo and co-workers found that UV irradiation could enhance the cytotoxicity of bare ZnO NPs and accelerate ROS generation in leukemia cell.[52] Yang *et al.* demonstrated that bare ZnO NPs significantly elevated the ROS level in primary mouse embryo fibroblast cells.[53] In fact, ZnO NPs are capable of inducing both spontaneous ROS generation and biological ROS generation.[51] There are inverse correlation between ROS and cell viability, and positive correlation between ROS and lactate dehydrogenase which is an indicator of cellular membrane integration.[17,51,54] In order to prove the ROS effects on the cell death in our research, ROS levels of Hela cells induced by ZnO@silica NPs were measured under UV light and visible light respectively. Compared with ZnO-A@silica and ZnO-B@silica, ZnO-C@silica induced a much higher ROS level under UV irradiation, while there was no significant difference in ROS level among these three products under visible light (see Fig. 7). Such significant difference under UV light was ascribed to the silica shell of ZnO-C@silica which is thinner and uncompleted, and ZnO-C@silica NPs are easier excite by 365 nm light to produce ROS. Therefore, our research suggests a way to kill cancer cells through uptaking ZnO@silica NPs under UV irradiation on one hand, and on the other, proves the well coated ZnO@silica NPs are safe for cellular experiments under visible light.

4. Conclusions

In summary, we have prepared monodispersed ZnO@silica NPs with blue, green and yellow emission through a three-step silanization using VTES, TEOS and APS as modification materials. The ZnO@silica NPs with surface amino groups displayed excellent stability and solubility in water, PBS and RPMI Medium 1640. These characteristics facilitate further modification with targeting ligands. The application as fluorescent probes of ZnO@silica NPs was explored through cellular uptake experiments of Hela cells. The ZnO@silica NPs exhibited low cytotoxicity and outstanding fluorescence stability *in vitro*, and thus can be further developed in biomedical applications.

Acknowledgements

This work was supported by the National Natural Science Foundation of China Research Project (grant no. 20873029, 20945002 and 20890022), NCET-11-0115, the Shanghai Committee of Science and Technology (grant no. 09QA1400400 and 09ZR1403900).

Notes and references

1 I. L. Medintz, H. T. Uyeda, E. R. Goldman and H. Mattoussi, *Nat. Mater.*, 2005, **4**, 435.
2 U. R. Genger, M. Grabolle, S. C. Jaricot, R. Nitschke and T. Nann, *Nat. Methods*, 2008, **5**, 763.
3 T. Jamiesona, R. Bakhshi, D. Petrovaa, R. Pococka, M. Imani and A. M. Seifalian, *Biomaterials*, 2007, **28**, 4717.
4 H. M. Xiong, *J. Mater. Chem.*, 2010, **20**, 4251.

5 Y. Y. Su, Y. He, H. T. Lu, L. M. Sai, Q. N. Li, W. X. Li, L. H. Wang, P. P. Shen, Q. Huang and C. H. Fan, *Biomaterials*, 2009, **30**, 19.
6 C. Wang, X. Gao and X. G. Su, *Talanta*, 2010, **80**, 1228.
7 K. Zierold, *Toxicol. in Vitro*, 2000, **14**, 557.
8 Y. Takano, T. Taguchi, I. Suzuki, J. U. Balis and K. Yuri, *Environ. Res., Sect. A*, 2002, **89**, 138.
9 E. A. Meulenkamp, *J. Phys. Chem. B*, 1998, **102**, 5566.
10 H. M. Xiong, R. Z. Ma, S. F. Wang and Y. Y. Xia, *J. Mater. Chem.*, 2011, **21**, 3178.
11 N. R. Jana, H. H. Yu, E. M. Ali, Y. G. Zheng and J. Y. Ying, *Chem. Commun.*, 2007, 1406.
12 M. Mortimer, K. Kasemets and A. Kahrua, *Toxicology*, 2010, **269**, 182.
13 K. Kasemets, A. Ivask, H. C. Dubourguier and A. Kahru, *Toxicol. in Vitro*, 2009, **23**, 1116.
14 M. Heinlaan, A. Ivask, I. Blinova, H. C. Dubourguier and A. Kahru, *Chemosphere*, 2008, **71**, 1308.
15 H. H. Wang, R. L. Wick and B. S. Xing, *Environ. Pollut.*, 2009, **157**, 1171.
16 V. Aruojaa, H. C. Dubourguier, K. Kasemetsa and A. Kahru, *Sci. Total Environ.*, 2009, **407**, 1461.
17 W. H. Song, J. Y. Zhang, J. Guo, J. H. Zhang, F. Ding, L. Y. Li and Z. T. Sun, *Toxicol. Lett.*, 2010, **199**, 389.
18 G. Applerot, A. Lipovsky, R. Dror, N. Perkas, Y. Nitzan, R. Lubart and A. Gedanken, *Adv. Funct. Mater.*, 2009, **19**, 842.
19 H. Yin and P. S. Casey, *Langmuir*, 2010, **26**, 15399.
20 A. Lipovsky, Z. Tzitrinovich, H. Friedmann, G. Applerot, A. Gedanken and R. Lubart, *J. Phys. Chem. C*, 2009, **113**, 15997.
21 X. S. Tang, E. S. G. Choo, L. Li, J. Ding and J. M. Xue, *Langmuir*, 2009, **25**, 5271.
22 L. H. Zhao and S. Q. Sun, *CrystEngComm*, 2011, **13**, 1864.
23 Y. S. Fu, X. W. Du, S. A. Kulinich, J. S. Qiu, W. J. Qin, R. Li, J. Sun and J. Liu, *J. Am. Chem. Soc.*, 2007, **129**, 16029.
24 H. M. Xiong, Y. Xu, Q. G. Ren and Y. Y. Xia, *J. Am. Chem. Soc.*, 2008, **130**, 7522.
25 S. Saliba, C. V. Serrano, J. Keilitz, M. L. Kahn, C. Mingotaud, R. Haag and J. D. Marty, *Chem. Mater.*, 2010, **22**, 6301.
26 C. A. Barnes, A. Elsaesser, J. Arkusz, A. Smok, J. Palus, A. Lesniak, A. Salvati, J. P. Hanrahan, W. H. de Jong, E. Dziubałtowska, M. Stepnik, K. Rydzynski, G. McKerr, I. Lynch, K. A. Dawson and C. V. Howard, *Nano Lett.*, 2008, **8**, 3069.
27 Z. M. Tao, B. B. Toms, J. Goodisman and T. Asefa, *Chem. Res. Toxicol.*, 2009, **22**, 1869.
28 T. Yu, A. Malugin and H. Ghandehari, *ACS Nano*, 2011, **5**, 5717.
29 J. S. Chang, K. L. B. Chang, D. F. Hwang and Z. L. Kong, *Environ. Sci. Technol.*, 2007, **41**, 2064.
30 M. A. C. Duarte, M. Giersig and L. M. L. Marzán, *Chem. Phys. Lett.*, 1998, **286**, 497.
31 Y. Sun, F. Masia, W. Langbein and P. Borri, *Phys. Status Solidi A*, 2009, **206**, 2822.
32 Y. Lu, Y. D. Yin, B. T. Mayers and Y. N. Xia, *Nano Lett.*, 2002, **2**, 183.
33 M. Q. Tan, Z. Q. Ye, G. L. Wang and J. L. Yuan, *Chem. Mater.*, 2004, **16**, 2494.
34 H. Yang, Y. M. Zhuang, H. Hu, X. X. Du, C. X. Zhang, X. Y. Shi, H. X. Wu and S. P. Yang, *Adv. Funct. Mater.*, 2010, **20**, 1733.
35 P. D. McNaughter, J. C. Bear, D. C. Steytler, A. G. Mayes and T. Nann, *Angew. Chem.*, 2011, **123**, 1.
36 Z. Q. Ye, M. Q. Tan, G. L. Wang and J. L. Yuan, *Anal. Chem.*, 2004, **76**, 513.
37 A. G. Martínez, J. P. Juste and L. M. L. Marzán, *Adv. Mater.*, 2010, **22**, 1182.
38 Y. H. Yang and M. Y. Gao, *Adv. Mater.*, 2005, **17**, 2354.
39 Y. Lu, Y. D. Yin, Z. Y. Li and Y. N. Xia, *Nano Lett.*, 2002, **2**, 785.
40 N. R. Jana, C. Earhart and J. Y. Ying, *Chem. Mater.*, 2007, **19**, 5074.
41 J. F. Wang, T. Tsuzuki, L. Sun and X. G. Wang, *ACS Appl. Mater. Interfaces*, 2010, **2**, 957.
42 R. O. Moussodia, L. Balan and R. Schneider, *New J. Chem.*, 2008, **32**, 1388.
43 R. O. Moussodia, L. Balan, C. Merlin, C. Mustind and R. Schneider, *J. Mater. Chem.*, 2010, **20**, 1147.
44 X. S. Tang, E. S. G. Choo, L. Li, J. Ding and J. M. Xue, *Chem. Mater.*, 2010, **22**, 3383.
45 H. Q. Shi, W. N. Li, L. W. Sun, Y. Liu, H. M. Xiao and S. Y. Fu, *Chem. Commun.*, 2011, **47**, 11921.
46 H. M. Xiong, D. P. Xie, X. Y. Guan, Y. J. Tan and Y. Y. Xia, *J. Mater. Chem.*, 2007, **17**, 2490.
47 E. A. Meulenkamp, *J. Phys. Chem. B*, 1998, **102**, 7764.
48 L. Y. Zhang, L. W. Yin, C. X. Wang, N. Lun, Y. X. Qi and D. Xiang, *J. Phys. Chem. C*, 2010, **114**, 9651.
49 Y. Y. Tay, T. T. Tan, F. Boey, M. H. Liang, J. Ye, Y. Zhao, T. Norby and S. Li, *Phys. Chem. Chem. Phys.*, 2010, **12**, 2373.
50 Y. Y. Tay, T. T. Tan, M. H. Liang, F. Boey and S. Li, *Phys. Chem. Chem. Phys.*, 2010, **12**, 6008.
51 T. Xia, M. Kovochich, M. Liong, L. Mädler, B. Gilbert, H. B. Shi, J. I. Yeh, J. I. Zink and A. E. Nel, *ACS Nano*, 2008, **2**, 2121.
52 D. D. Guo, C. H. Wu, H. Jiang, Q. N. Li, X. M. Wang and B. A. Chen, *J. Photochem. Photobiol., B*, 2008, **93**, 119.
53 H. Yang, C. Liu, D. F. Yang, H. S. Zhang and Z. G Xi, *J. Appl. Toxicol.*, 2009, **29**, 69.
54 C. C. Huang, R. S. Aronstam, D. R. Chen and Y. W. Huang, *Toxicol. in Vitro*, 2010, **24**, 45.